Environmental Pollution 307 (2022) 119547

Contents lists available at ScienceDirect

Environmental Pollution

journal homepage: www.elsevier.com/locate/envpol

Spatial distribution of microplastics in the tropical Indian Ocean based on laser direct infrared imaging and microwave-assisted matrix digestion☆

Lars Hildebrandt [a,1], Fadi El Gareb [a,b,1], Tristan Zimmermann [a], Ole Klein [a,c], Andreas Kerstan [d], Kay-Christian Emeis [a,b], Daniel Pröfrock [a,*]

[a] Department for Inorganic Environmental Chemistry, Helmholtz-Zentrum Hereon, Max-Planck-Straße 1, 21502, Geesthacht, Germany
[b] Department of Geoscience, Institute of Geology, Universität Hamburg, Bundesstraße 55, 20146, Hamburg, Germany
[c] Department of Chemistry, Inorganic and Applied Chemistry, Universität Hamburg, Martin-Luther-King-Platz 6, 20146, Hamburg, Germany
[d] Agilent Technologies Sales & Services GmbH & Co. KG, Hewlett-Packard-Straße 8, 76337, Waldbronn, Germany

ARTICLE INFO

Keywords:
Large-scale microplastic study
Fractionated filtration
Quantum cascade laser
LDIR Imaging
One-pot digestion
Method development

ABSTRACT

Suspended particulate matter was collected from subsurface (6 m) water along an E-W transect through the tropical Indian Ocean using a specialized inert (plastic free) fractionated filtration system. The samples were subjected to a new microwave-assisted "one-pot" matrix removal (efficiency: 94.3% ± 0.3% (1 *SD*, $n = 3$)) and microplastic extraction protocol (recovery: 95% ± 4%). The protocol enables a contamination-minimized digestion and requires only four filtration steps. In comparison, classical sample processing approaches involve up to eight filtration steps until the final analysis. Microplastics were identified and physically characterized by means of a novel quantum cascade laser-based imaging routine.

LDIR imaging facilitates the analysis of up to 1000 particles/fibers (<300 μm) within approximately 1–2 h. In comparison to FTIR and Raman imaging, it can help to circumvent uncertainties, e. g. from subsampling strategies due to long analysis and post-processing times of large datasets. Over 97% of all particles were correctly identified by the automated routine - without spectral reassignments. Moreover, 100% agreement was obtained between ATR-FTIR and LDIR-based analysis regarding particles and fibers >300 μm.

The mean microplastic concentration of the analyzed samples was 50 ± 30 particles/fibers m^{-3} (1 *SD*, $n = 21$). Number concentrations ranged from 8 to 132 particles/fibers m^{-3} (20–300 μm). The most abundant polymer clusters were acrylates/polyurethane/varnish (49%), polyethylene terephthalate (26%), polypropylene (8%), polyethylene (4%) and ethylene-vinyl acetate (4%). 96% of the microplastic particles had a diameter <100 μm. Though inter-study comparison is difficult, the investigated area exhibits a high contamination with particulate plastics compared to other open ocean regions. A distinct spatial trend was observed with an increasing share of the size class 20–50 μm from east to west.

1. Introduction

Microplastic (MP) particles (1 μm - 5 mm (Frias and Nash, 2019)) can be considered an omnipresent (emerging) contaminant. Synthetic polymeric particles were detected in a plethora of terrestrial (Mai et al., 2018; Scheurer and Bigalke, 2018), marine (Bergmann et al., 2017; Lorenz et al., 2019), riverine (Mani et al., 2015; Scherer et al., 2020), atmospheric (Brahney et al., 2021; Dris et al., 2016) or biological samples (Fischer and Scholz-Böttcher, 2017; Thiele et al., 2021). Over 10% of the plastic debris in the ocean surface layer are assigned to ingestible and potentially harmful MPs. Besides primary MPs, so-called secondary MPs are formed by UV-induced, mechanical or biological degradation of larger debris (Song et al., 2017). In the last years, advanced analytical methods focusing on particulate plastics were developed and validated (Bannick et al., 2019; Becker et al., 2020; Duemichen et al., 2019; Hildebrandt et al., 2020b; Hildebrandt et al., 2019; Kirstein et al., 2021; Löder et al., 2017; Mitrano et al., 2019; Primpke et al., 2017).

From a regulatory perspective, the US state California has a vanguard

☆ This paper has been recommended for acceptance by Maria Cristina Fossi.
* Corresponding author.
E-mail address: daniel.proefrock@hereon.de (D. Pröfrock).
[1] Equally contributing first-authors.

https://doi.org/10.1016/j.envpol.2022.119547
Received 5 November 2021; Received in revised form 23 May 2022; Accepted 24 May 2022
Available online 28 May 2022

role regarding the planned regulation of MPs in drinking water (Senate Bill No. 1422). Nevertheless, there are also topical endeavours to fight (micro)plastic pollution on a global scale, e.g. by the UN Sustainable Development Goals (Walker, 2021) or the EU Marine Strategy Framework Directive. In a prominent perspective article, Mitrano and Wohlleben (2020) stated that "the recent MP definitions proposed by European Chemical Agency for a potential restriction of solid primary MPs via the REACH regulation (EU law for Registration Evaluation, Authorization and Restriction of Chemicals) goes far beyond the original scope of banning the microbead campaigns". However, for monitoring of environmental compartments and compliance with restrictions as proposed by the ECHA (European Chemical Agency, 2019), time-efficient, automatable and validated chemical-analytical and data processing workflows are indispensable.

From the perspective of routine laboratories, established sample preparation methods, as well as the microspectroscopic detection of MPs are still too labor-intensive, time-consuming, and dependent on the skills of the operator (Hüffer et al., 2017; Huppertsberg and Knepper, 2018; Müller et al., 2020; Primpke et al., 2020a; Stock et al., 2020).

Recently, external cavity quantum cascade laser (QCL) imaging proved its high potential for MP analysis, in terms of both time-efficiency and reliability (Hildebrandt et al., 2020a; Li et al., 2021b; Primpke et al., 2020b; Scircle et al., 2020). QCLs are rapidly and broadly tunable semiconductor lasers emitting in the mid-infrared region of the electromagnetic spectrum (Doulamis et al., 2021; Kuepper et al., 2018). As Fourier transformation is omitted, the acquisition of IR spectra is tremendously faster compared to state-of-the-art FTIR microscopes (up to 150-times faster at an equivalent signal-to-noise ratio) (Ogunleke et al., 2017). Additionally, the higher peak signals of such QCL systems compared to broadband sources has a positive effect on the sensitivity (Childs et al., 2015; Primpke et al., 2020b).

Environmental filtration and bulk samples, such as sediment, sewage sludge or biological tissue, usually contain large amounts of a complex mixture of biogenic, mineral and/or organic material. Therefore, validated and time efficient sample preparation protocols are needed when applying spectroscopic methods for MP detection. Various protocols comprise a sequence of chemical (HNO_3, NaOH, KOH, NaOCl, H_2O_2, sodium dodecyl sulfate (SDS)) and/or enzymatic (protease, cellulose, lipase, chitinase) treatments in order to remove natural (polymeric) matrix components (Cutroneo et al., 2020; Löder et al., 2017; Lorenz et al., 2019; Miller et al., 2017; Thiele et al., 2019). Digestion at different temperatures (Munno et al., 2018) and usage of in-house-built devices (Coppock et al., 2017; Löder et al., 2017) are also common practice. However, many approaches suffer from poor recoveries, detrimental effects on MP integrity and procedural contamination problems (Koelmans et al., 2019; Prata et al., 2021; Wang et al., 2018). This can lead to biased or false positive results. Accordingly, inter-study comparability is hampered. Furthermore, many studies lack method validation. Currently, no certified reference materials (CRMs) for MP analysis are available to evaluate the performance of the different sample preparation protocols in a comparable and traceable way.

The aim of this study was the development and application of two innovative analytical tools for the determination of MPs in the Indian Ocean. In this context, we developed a new, time efficient enzymatic-oxidative microwave-assisted "one pot" matrix removal protocol. The matrix removal was followed by analysis of the MPs by powerful state-of-the-art laser direct infrared (LDIR) imaging. The developed protocol was applied to 21 subsurface samples from the tropical Indian Ocean. This study deals with a large marine area for which, on the one hand, there is a very poor data situation. On the other hand, the investigated area is expected to be highly contaminated as the transect followed low salinity water masses of Indonesian Throughflow Water fed by large rivers in Asia.

2. Materials and methods

2.1. Geesthacht Inert Microplastic Fractionator

The Geesthacht Inert Microplastic Fractionator is a sampling system for online-size-fractionation of particles from a liquid medium. It consists of two channels with two 19 ¾ inch stainless-steel cartridge filters each (300 μm and 10 μm mesh size, Wolftechnik Filtersysteme, Weil der Stadt, Germany). The entire unit is made of stainless-steel (pipe system: AISI 316 L steel, Swagelok, Ohio, USA). All sealings are perfluoroalkoxy alkane-sheathed to avoid contamination with relevant plastics. On the backside, a calibrated flow meter (RS Components GmbH, Frankfurt am Main, Germany), as well as a fifth cartridge filter (2 μm mesh size, Wolftechnik Filtersysteme) is mounted. This filter can be used for backflushing the entire system with filtered freshwater after each sampling. Detailed pictures of the Geesthacht Inert Microplastic Fractionator can be found in SI Fig. 1.

2.2. Sampling

The Geesthacht Inert Microplastic Fractionator was applied on board of the German research vessel Sonne (SO270 cruise, MASCARA) to conduct volume-reduced MP sampling ($V_{mean} = 1.34$ m^3; 0.74–5.71 m^3) along a transect in the Indian Ocean from Hong Kong to Port Louis. In total, 2 × 21 samples ($d > 300$ μm and 10 μm $\leq d \leq 300$ μm, respectively) were taken at 21 locations between 98°E to 64°E and 7°S to 13°S. GPS coordinates of all sampling locations are listed in SI Table 1.

The Geesthacht Inert Microplastic Fractionator enabled the filtration of high amounts of suspended particulate matter (SPM) ($d_{SPM} \geq 10$ μm) by being fed with water from the ship's moon pool at 6 m below sea level. The water was pumped by a submersed pump (stainless steel, $d =$ 5 inch, $F \leq 5$ m^3 h^{-1}, Lowara model SC207C, Xylem Deutschland,

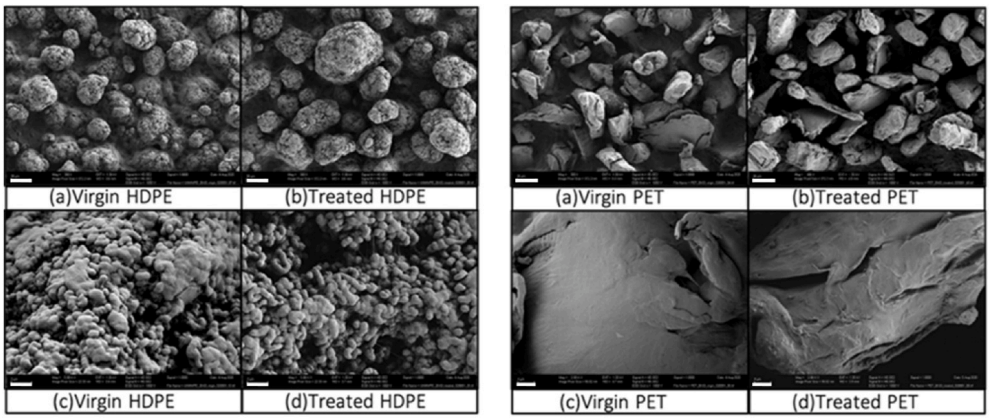

Fig. 1. Left: SEM images of (a): virgin HDPE particles with 300× magnification, scale bar = 30 μm; (b): treated HDPE particles with 300× magnification, scale bar = 30 μm; (c): single virgin HDPE particle with 5000× magnification, scale bar = 2 μm; (d): single treated HDPE particle with 5000× magnification, scale bar = 2 μm. Right: SEM images of (a): virgin PET particles with 300× magnification, scale bar = 30 μm; (b): treated PET particles with 300× magnification, scale bar = 30 μm; (c): single virgin PET particle with 2000× magnification, scale bar = 4 μm; (d): single treated PET particle with 2000× magnification, scale bar = 4 μm.

Table 1
Mass reduction results for particulate reference matrices (Plankton CRM and German Elbe River SPM). Mass values are given for plankton CRM (BCR-414; 200 mg) and Elbe River SPM (125 mg). The entire matrix removal protocol includes all digestion steps in the "one-pot approach" and the subsequent density separation with $ZnCl_2$ solution (1 *SD*, $n = 3$ for all results).

mass [mg]	reagents	vol. [mL]	temp. [°C]	pH	time [h]	mass reduction [%]
200	Proteinase K (1.5 mg) dissolved in 2 mL Tris - HCl buffer solution + 1 mL SDS solution (1.5% (*w/w*))	3	37	8.5	2	44 ± 4
200	6 mL H_2O_2 15% (*v/v*) + $FeSO_4$ ($c = 6.6$ mg mL^{-1}, 0.2 mL)	6.2	50	–	0.5	45.6 ± 0.5
200	4 mL Chitinase + 6 mL Acetic acid/sodium acetate buffer solution	10	40	5.0	24	50.3 ± 0.5
125	**entire matrix removal protocol (digestion + density separation)**	**19.2**	**-**	**-**	**216**	**94.3 ± 0.3**

Langenhagen, Germany) via a polytetrafluoroethylene (PTFE)-lined hose (DIEFLEX Chemieschlauch PTFE-SD white, DIEFLEX technische produkte, Barsbüttel, Germany). Seawater was pumped through the filtration unit for about half an hour at an average ship speed of 10 knots along straight routes.

Afterwards, the individual filter cartridge, as well as the water inside the housing was transferred quantitatively into a glass beaker. 2 mL of pre-filtered SDS solution (10% (*w/w*), Fisher Scientific) were added to the seawater remaining in the housings. The filters were ultrasonicated for max. 30 s in the respective seawater (approx. 2 L). The resulting suspension was filtered over PTFE membranes ($d = 47$ mm, 5 μm pore size, Sartorius AG, Goettingen, Germany) using borosilicate glass vacuum filtration units (Merck KGaA, Darmstadt, Germany).

The membranes were stored in wide neck bottles (amber glass) under cold and dark conditions in 100 mL filtered Milli-Q water (MQW). 1 mL of pre-filtered 30% (*w/w*) HCl (practical grade, Carl Roth GmbH + Co. KG, Karlsruhe, Germany) was added for conservation ($c_{HCl} = 0.3\%$ (*v/v*)). A procedural blank was conducted on board of the research vessel by filtering approx. 1 m^3 of ship's distilled water.

2.3. Contamination mitigation

A strict protocol was followed in order to prevent contamination from the sampling equipment, laboratory equipment, reagents, clothing and airborne sources. This included the rigorous use of laminar flow benches class II (inside the laboratory and on board of the research vessel), filtration of all reagents, the use of cleaned metal or glass laboratory equipment and the conduction of method blanks. A more detailed description of the conducted contamination mitigation procedures can be found in SI chapter 1.2.

2.4. Microwave-assisted enzymatic-oxidative matrix digestion and density separation

In the laboratory, samples were quantitatively transferred into 400 mL glass beakers and ultrasonicated for 30 s. The entire sample suspension was subsequently transferred onto a 5 μm PTFE filter via vacuum filtration (Merck KGaA, Darmstadt, Germany). Membranes were transferred into 35 mL microwave quartz pressure vessels (CEM GmbH, Kamp-Lintfort, Germany). 1.5 mg Proteinase K powder (from *Tritirachium album*, 3.0 U mg^{-1} - 15 U mg^{-1}, Merck KGaA, Darmstadt, Germany, $c = 500$ μg mL^{-1}) dissolved in 2 mL *tris*-(hydroxymethyl)-aminomethane-HCl buffer solution ($c = 0.2$ mol L^{-1}, pH = 8.5) and 1 mL SDS solution (1.5% (*w/w*)) were added (after pre-filtration).

Samples were incubated for 2 h at 37 °C on a hotplate (EasyDigest monobloc, Analab, Hoenheim, France). Afterwards, samples were incubated for 0.5 h in 6 mL of H_2O_2 (15% (*v/v*)) (by addition of 3 mL of 30% (*v/v*) H_2O_2) at 50 °C in a laboratory microwave system (Discover SP-D 35, CEM GmbH, Kamp-Lintfort, Germany). 0.2 mL of Fe^{2+} catalyst solution $FeSO_4$ ($c = 6.6$ mg mL^{-1}) was added to degrade the remaining H_2O_2 by forming free hydroxyl and hydroperoxyl radicals. This mechanism is commonly known as *Fenton* reaction. 4 mL of Chitinase (from *Trichoderma harzianum*, > 150 U mg^{-1}, ASA Spezialenzyme GmbH, Wolfenbüttel, Germany) and 6 mL of an acetic-acid/sodium acetate (both Merck KGaA, Darmstadt, Germany) buffer solution ($c = 1$ mol L^{-1}, pH = 5.6) was added to the vessel. The second enzymatic treatment was carried out on a hotplate for 24 h at 37 °C. A second filtration step was conducted to subsequently rinse lithogenic material and MPs into a separator funnel containing pre-filtered $ZnCl_2$ solution ($\rho = 1.7$ g mL^{-1}, Merck KGaA, Darmstadt, Germany). After two to seven days, the upper phase (including MPs), was passed through 5 μm PTFE membranes via vacuum-filtration. The glass funnel was rinsed with both MQW and HCl (4% (*v/v*)), in order to remove small precipitates of $ZnCl_2$. Used $ZnCl_2$ solution was recycled three times by filtration through 1 μm glass fiber filter membranes (Sartorius AG, Göttingen, Germany). Purified samples (particle size fraction <300 μm) were re-suspended with approx. 5 mL ethanol (50% (*v/v*)) in a cleaned glass Petri dish ($d = 50$ mm). Finally, the entire samples were deposited on MirrIR (low-e microscope) slides (Kevley Technologies, Chesterland, USA) using a 1 mL glass pipette.

2.4.1. Determination of the digestion efficiency

Digestion efficiency was gravimetrically determined for each tested agent by vacuum filtration of digested plankton CRM (BCR-414, Joint Research Centre, Geel, Belgium) onto pre-weighted polycarbonate (PC) filter membranes (0.4 μm). All mass calculations refer to the dry weight (*DW*). Therefore, the filter membranes were dried at 30 °C for 24 h.

Digestion efficiencies were calculated using the following equation:

$$Digestion\ efficiency\ (\%) = \left(1 - \frac{m_1 - x}{m_2 - y}\right) * 100\%$$

$m_1 = DW$ of CRM on filter membrane after filtration (mg)
m_2 = mass of CRM used for filtration (mg)
$y = DW$ of CRM found in filtrate (mg)
x reagent mass effect (mg)

Calculation of reagent mass effect x:

$$x = m_3 - m_4$$

$m_3 = DW$ of filter membrane after reagent filtration (mg)
$m_4 = DW$ of filter membrane before reagent filtration (mg)

Reagent mass effects were calculated from triplicate filtration (1 *SD*, $n = 3$): For Proteinase K: 0.04 mg ± 0.01 mg, for *Fenton* reagent (combination of H_2O_2 and Fe^{2+}): 3.63 mg ± 0.12 mg, for Chitinase: 0.30 mg ± 0.02 mg.

2.4.2. Determination of recovery rates

Recovery rates of the optimized workflow were determined by using in-house reference MPs (high-density polyethylene (HDPE) ($\rho = 0.94$ g mL^{-1}) and polyethylene terephthalate (PET) ($\rho = 1.3$ g mL^{-1} - 1.4 g mL^{-1}), ($d = 20$ μm–63 μm)). The polymer particles were received as plastic powders (Goodfellow GmbH, Hamburg, Germany) and sieved using a stainless-steel sieving cascade (AS300, Retsch GmbH, Haan, Germany). Recovery rates were determined in triplicates on a gravimetric basis. 200 mg of the MP powders were vacuum-filtrated onto pre-weighed PTFE membranes with MQW. The PTFE membranes containing

the reference MPs were subjected to the optimized digestion and density separation protocol.

Afterwards, the particles were enriched onto pre-weighed PTFE membranes and dried at 30 °C for 24 h. ATR-FTIR and LDIR spectra of the polymer powders were recorded before and after digestion and density separation. Furthermore, scanning electron microscopy (SEM, Gemini, Carl Zeiss Microscopy Deutschland GmbH, Jena, Germany) was applied to discover potential changes of the surface structure. Recovery rates were calculated using the following equation:

$$Recovery\ (\%) = \frac{m_5}{m_6} * 100\%$$

$m_5 = DW$ of MP powder after digestion (mg)
$m_6 = DW$ of MP powder before digestion (mg)

2.5. Sample preparation and analysis of microplastics >300 μm

2.5.1. Sample preparation

Visual inspection and sorting was applied to the larger size fraction, according to a protocol adapted from Lorenz et al. (2019). Before their transfer into a *Bogorov* counting chamber (poly(methyl methacrylate) (PMMA); 70 mL capacity, HydroBios, Kiel, Germany), samples were ultrasonicated for 30 s. PTFE filters and glass bottles were rinsed three times with MQW and Ethanol (50% (*v/v*)) into the counting chamber. Suspensions and PTFE filters were visually inspected under a stereomicroscope (Olympus SZ61, Olympus Europa SE & Co. KG, Hamburg, Germany) at 1.2- to 4.5-fold magnification. Potential MPs were sorted with metal tweezers and stored in a *Gollasch* counting chamber (PMMA, 30 fields capacity, HydroBios, Kiel, Germany). All particles with a bright or transparent color and without cellular structures were isolated and photographed (Altra 20 Soft Imaging System, Olympus Soft Imaging Solutions GmbH, Münster, Germany). Particles were measured at their longest and shortest dimension using the camera-specific imaging software (AnalySIS, Olympus Soft Imaging Solutions GmbH, Münster, Germany).

2.5.2. Sample analysis

Potential large MP particles and fibers were analyzed by ATR-FTIR spectroscopy (Alpha I, Bruker Optics, Ettlingen, Germany) (on a diamond or germanium crystal). Measurements were performed three times with 32 scans and a resolution of 4 cm^{-1} (wavenumber range: 4000 cm^{-1} – 400 cm^{-1}). The respective spectra were compared to the siMPle database developed by Primpke et al. (2020a) (https://simple-plastics.eu). Assignments with hit quality values > 700/1000 were automatically accepted. Assignments between 700/1000 and 550/1000 were re-evaluated based on expert knowledge. For comparison purposes, detected large MP particles were additionally analyzed using an Agilent 8700 LDIR Chemical Imaging system (Agilent Technologies, Santa Clara, USA) using both transflection mode and μ-ATR analysis. One representative blue fiber was also analyzed by μ-Raman spectroscopy (Senterra, Bruker Optik GmbH, Ettlingen, Germany). Raman spectra were compared to the Pigments-Checker database.

2.6. Sample preparation and analysis of microplastics <300 μm

2.6.1. Sample preparation

The samples were subjected to the newly developed microwave-assisted "one-pot" enzymatic-oxidative digestion protocol using Proteinase K and SDS, H_2O_2 and Fe^{2+} catalyst, and Chitinase (for details see chapter 2.4.).

2.6.2. Sample analysis

The sample fraction <300 μm was analyzed using the Agilent 8700 LDIR Chemical Imaging system (Agilent Technologies) in transflection mode. The instrument's functional principles are described in more detail in previous publications (da Costa Filho et al., 2020; Dong et al., 2022; Hildebrandt et al., 2020a; Scircle et al., 2020). The particle analysis workflow of the Agilent Clarity software (version 1.1.2) was used for the automated analysis of the entire sample set. Hereby, the sensitivity was set to the maximum (6/6).

Spectra were acquired with a spectral resolution of 8 cm^{-1}. The particle size range of the LDIR imaging system was generally set to 20 μm–5000 μm according to the presets of the software. The automatic workflow of the LDIR technically enables MP detection down to 10 μm. However, the practically achievable size detection limit highly depends on the analyzed matrix and the level of cleanliness of the sample.

The used spectral library (Microplastic starter 1.0, Agilent Technologies) was expanded by spectra of relevant environmental particles (confirmed with the μ-ATR-unit of the system) obtained from natural matrices (plankton CRM BCR-414, as well as SPM from the German Elbe River and North Sea). Natural matrices contributed a variety of spectra relevant for the analysis of MPs in the presented sample set. Additionally, the spectra of in-house reference MPs (expanded polystyrene (EPS), polyethylene (PE), polyethylene terephthalate (PET), polypropylene (PP), polystyrene (PS) and polyvinylidene chloride (PVDC)) and different polymeric materials used in the laboratory were integrated into the library.

The automated workflow of the Clarity software acquired IR spectra for all particles. The hit quality thresholds for a positive assignment were adapted according to the preset values. MP identifications were either accepted, manually assigned to another polymer class, or not accepted. Only spectra in conjunction with high hit quality values related to reference spectra (>0.80) were considered for the final statistics without further manual confirmation. In order to prevent any overestimation of the MP concentrations, all analyses were thoroughly re-evaluated manually in transflection mode and, if necessary, also by the LDIR's μ-ATR function. If unambiguous confirmation of the assignment was not possible, the respective particles were assigned to natural material classes or marked as "unknown". Particles with hit qualities <0.60 were automatically classified as "unknown".

3. Results and discussion

3.1. Enzymatic-oxidative sample preparation protocol

3.1.1. Matrix digestion

In the method development phase, the digestion efficiencies of different digestion steps using Proteinase K, Chitinase, as well as *Fenton* reagent were determined (see Table 1). Validation was based on treatment of typical marine SPM. A matrix-matched CRM was utilized (BCR-414, PLANKTON (trace elements)). The mass of plankton CRM was adjusted to 200 mg corresponding to average SPM concentrations in surface waters of the tropical Indian Ocean ($C_{SPM} = 0.25$ g m^{-3}).

The highest isolated matrix reduction was observed for the Chitinase treatment. During this step, the sample mass was reduced by 50.3% ± 0.5% (1 *SD*, $n = 3$). Proteinase K in conjunction with SDS showed a mass reduction of 44% ± 4%. Experiments demonstrated that *Fenton* reagent leads to an increased mass reduction of 45.6% ± 0.5% by degrading organic material more rapidly than 15% H_2O_2 (*v/v*) alone. The overall digestion protocol achieves a nearly quantitative matrix reduction of 94.3% ± 0.3%. This is comparable to established protocols based on the use of alkalines or acids. KOH digestion at temperatures between 25 °C and 40 °C may even achieve efficiencies between 97% and 98% (Karami et al., 2017).

The presented digestion can be carried out in less than 9 days. This is still a high time demand but significantly faster than other basic enzymatic purification protocols, e.g. developed by Löder et al. (2017), which takes around 16 days and 8 filtration steps to accomplish. The developed protocol only applies four filtration steps in total. This reduces the workload and minimizes the risks of contamination, e.g. by airborne particles, or sample loss. The usage of controlled

Table 2
Results of the recovery experiments. All recovery rates are referred to the mass of model MP particles (1 *SD*, $n = 3$).

reference particles (d = 20–63 μm)	mass [mg]	treatment	recovery [%]
model HDPE particles	200	none/MQW suspension	98.0 ± 1.1
model PET particles	200	none/MQW suspension	99.0 ± 0.3
model HDPE particles	200	entire matrix removal protocol	95 ± 4
model PET particles	200	entire matrix removal protocol	98.3 ± 0.3

microwave-assisted heating allows fast energy transfer and more reproducible conditions. The temperature inside the closed reaction vessels is continuously monitored during the digestion procedure. This will be helpful in particular to develop harmonized, traceable and more reproducible sample preparation protocols in the near future.

3.1.2. Microplastic recoveries and surface morphology

The digestion protocol was also validated in terms of recoveries - analogously to Hildebrandt et al. (2021). Table 2 shows the results of the recovery experiments: Model MP particles after suspension in MQW and running through the matrix removal protocol.

In total, 98.0% ± 1.1% of HDPE and 99.0% ± 0.3% of PET particles were recovered after vacuum filtration onto 5 μm PTFE filter membranes. 95% ± 4% of HDPE particles were recovered after the entire matrix removal protocol, including all four filtration steps. PET particles exhibited a corresponding recovery rate of 98.3% ± 0.3%.

Although model MPs used in this study exhibit different buoyancies in water (PE: 0.89–0.98 g cm^{-3}; PET: 1.38–1.41 g cm^{-3}), recovery rates for HDPE and PET do not differ significantly. Prevention of particle loss is more difficult regarding HDPE due to its higher hydrophobicity compared to PET. This may explain the slightly higher variation of HDPE recoveries. Additionally, it was assured that the entire protocol does not have any detrimental effects on MPs. The treated and untreated particles were investigated by means of SEM (see Fig. 1) indicating no significant difference in surface morphology and particle integrity. ATR-FTIR and LDIR analysis of the particles before and after the treatment did not reveal any changes in the IR spectra. Burns and Boxall state that "there is, however, a mismatch between the particle types, size ranges, and concentrations of microplastics used in laboratory tests and those measured in the environment" (Burns and Boxall, 2018).

Indeed, recoveries rates are either determined by weighing MPs <100 μm (Bordós et al., 2021; Möller et al., 2022) or counting MPs >100 μm (Dimante-Deimantovica et al., 2022; Funck et al., 2020; López-Rosales et al., 2022). That reproducible spiking of low numbers of MPs <100 μm is highly challenging explains this trade-off.

3.1.3. Remaining natural matrix constituents in real samples

After matrix digestion, 97.7% of all detected particles were natural (polymeric) materials present in the seawater SPM matrix (cellulosic, silicate, coal, chitin and natural polyamide). Only 2.3% of all particles were MPs. Fig. 2 provides an overview of some of the remaining natural components in the samples after matrix reduction.

As some planktonic species such as diatoms and radiolaria build their shells out of silica, they are not fully decomposed by enzymatic digestion steps. They were partly removed by means of density separation, but their removal was not quantitative.

3.1.4. Blanks

No MPs were found in the procedural blanks ($n = 4$). These were run simultaneously to the treatment of the size fraction 10 μm ≤ d ≤ 300 μm. Nonetheless, non-plastic fibers were found ($n = 9$), which probably stem from non-synthetic clothing worn during the laboratory work. Therefore, no quantitative correction was made to the MP numbers. Fibers of similar appearance were also found in various samples and classified as non-plastic.

Strict work in laminar flow clean benches (on board of the research vessel and in the laboratory) and usage of HEPA air filters inside the lab explains the lower share of synthetic microfibers compared to other studies. Wesch et al. (2017) have experimentally shown that pollution by microfibers has been overestimated in the past as many researchers did not use laminar flow clean benches. Moreover, no carryover effects were observed. Vials used for sample digestion were randomly used for subsequent procedural blanks (after the cleaning procedure).

3.2. Microplastic distribution in the tropical Indian Ocean

Even though a high level of contamination and possible effects on the environment are likely (Li et al., 2021a; Patti et al., 2020; van der Mheen et al., 2020), there is only poor data on MP contamination of the Indian Ocean compared to the other ocean regions. Schmidt et al. (2017) assumed that eight of the ten rivers responsible for 90% of the plastic discharges into the oceans are located in Asia. Thus, the Indian Ocean's MP levels are considered as highly influenced by inputs from rivers with the prevailing westward transport by relatively fresh surface waters of the Indonesian Throughflow. Additionally, China, India, Bangladesh and Vietnam account for ~50% of the global textile and apparel production (Agarwal et al., 2017). As environmental microfiber release also occurs during the production process (Henry et al., 2019), high levels of fiber contamination are expectable for Asian rivers and marine waters.

3.2.1. Microplastics >300 μm in the tropical Indian Ocean

The collected SPM fraction >300 μm referring to a total volume of 27.97 m^3 was visually inspected. Only three particles were confirmed to be MPs (1 PP and 2 PET). One particle was classified as mesoplastic. The resulting mean MP concentration for the fraction >300 μm is 0.1 ± 0.4 MP m^{-3} and herewith in the range of other reports. Doyle et al. (2011) reported similar amounts of larger MPs (>500 μm) in subsurface waters of the Northeast Pacific Ocean (0.19 MP m^{-3}). Furthermore, MP concentrations in the large MP fraction are comparable to findings by Lorenz et al. (2019) for coastal surface waters of the North Sea (0.05–4.42 MP m^{-3} for MPs >500 μm). Numerical model calculations with respect to concentrations of larger MP particles within marine environments (>500 μm) by Kooi et al. (2016) demonstrated a rapid decrease below

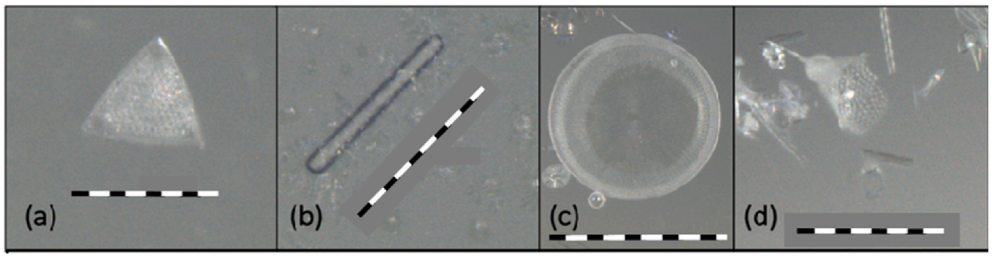

Fig. 2. High magnification images of planktonic species remaining on the MirrIR slide after digestion and density separation, recorded with the microscope objective of the LDIR: (a) triangular shaped diatom (scale bar = 100 μm); (b) pennate diatom (scale bar = 150 μm); (c) centric diatom (scale bar = 250 μm) and (d) radiolaria (scale bar = 100 μm).

1.5 m water depth. Thus, MP concentrations at the water surface may be significantly higher than in subsurface waters (6 m sampling depth in this study).

Our results are well in line with other studies which have demonstrated that representative sampling of MPs >300 μm requires filtration of large volumes (Bannick et al., 2019; Karlsson et al., 2020; Tamminga et al., 2019).

Significantly higher amounts of blue anthropogenic fibers (3.2 ± 1.7 fibers m^{-3}) were detected compared to large MP particles (0.1 ± 0.4 MP m^{-3}). Raman analysis revealed the presence of Indigo blue. Indigo blue is frequently used to dye textile fibers, e.g. made of cotton. The ubiquitous presence of such anthropogenic fibers (synthetic and cellulosic ones) in marine environments is attributed to their release from garments during washing (Cole, 2016). Fibers can finally reach the marine environment through rivers or as airborne inputs (Suaria et al., 2020). The higher production volumes of synthetic fibers compared to natural fibers is at odds with the higher occurrence of natural textile fibers in the water column of the tropical Indian Ocean. Of > 100 million tons of fibers produced in 2017, 60% were synthetic, 30% cotton and 10% other fibers (Reineccius et al., 2020). Nonetheless, our results are in accordance with other studies which indicate that synthetic polymers only account for a small portion of the total amount of fibers in marine environments (Suaria et al., 2020). Density differences (PET is comparably heavy, > 1.38 g cm^{-3}), different sizes, but also the fact that synthetic fibers have not been used for very long time are possible explanations.

3.2.2. *Microplastics <300 μm in the tropical Indian Ocean*

MP concentrations in the size range 20–300 μm span from 8 to 132 particles/fibers m^{-3} (average: 50 ± 30 MPs m^{-3} (1 *SD*, $n = 21$)). Fig. 3 shows the spatial distribution of measured number concentrations. Furthermore, detailed results of the LDIR imaging analysis are listed in SI Table 2. The minimum of particles required for concentration comparisons according to Karlsson et al. (2020) (assuming Poisson distribution) was exceeded at 18 out of 21 stations.

The highest concentrations were measured at station 4 (132 particles/fibers m^{-3}) and station 11 (124 particles/fibers m^{-3}). Three stations (1, 2 and 7) exhibited concentrations ranging between 5 and 20 particles/fibers m^{-3}.

Before putting these number into the context of other studies, we stress that MP number concentrations reported in different articles are depended on the entire analytical workflow, including the sampling size cut-off, sampling depth, filters used during sample processing, contamination prevention measures, the chemicals used for matrix removal and the imaging and data evaluation processes. In a study by Kooi et al. (2016), marine MP concentrations were on average nine times lower in a depth between 0 and 5 m compared to the corresponding surface waters. In the East Indian Ocean, low mean MP concentrations of 1.3 ± 0.6 MPs m^{-3} (1 *SD*) were reported for surface waters, 1.3 ± 1.0 MPs m^{-3} for intermediate waters and 1.3 ± 0.4 MPs m^{-3} for halocline waters (Li et al., 2020). This can be explained by the comparably high size cut-off (62 μm) applied by Li et al. (2020). This excludes >75% of the MPs found in our study.

The patterns of MP abundances along the E-W transect and variability in MP types encountered are not consistent with an exclusive origin from large river sources of MP in Asia and advection with low-salinity surface water of the Indonesian Throughflow. Instead, the abundance and polymer patterns suggest a predominantly regional or even local origin. The data do not reflect postulated very high MP

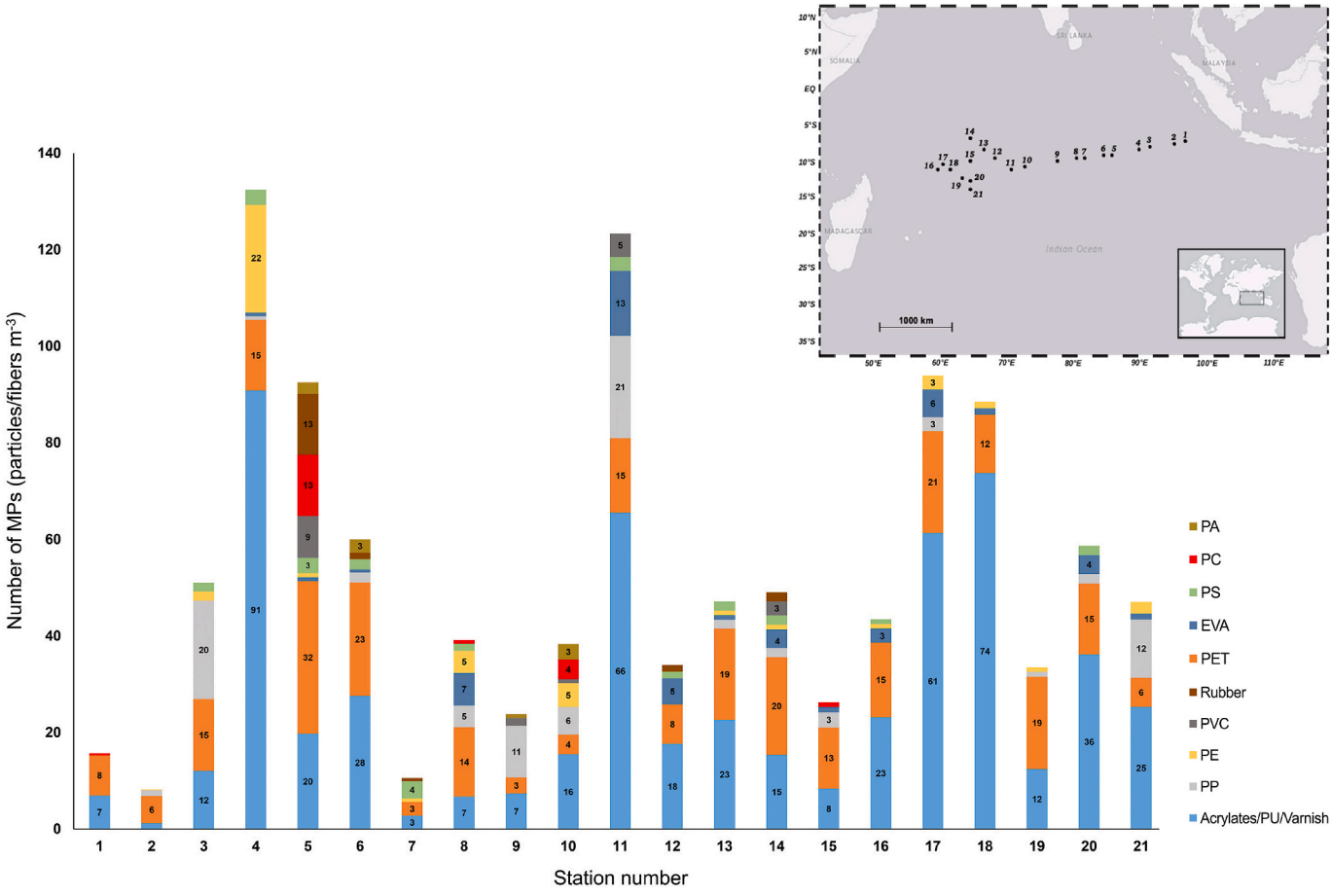

Fig. 3. MP number concentrations and polymer compositions for the different stations in the tropical Indian Ocean. Most abundant polymer clusters are displayed. PE-Cl, PMMA, acrylonitrile butadiene and silicone quantities are not displayed (<3 particles/fibers m^{-3}).

concentrations for the southern Indian Ocean gyre that is estimated to carry the highest debris concentrations among all Ocean regions of the southern hemisphere (Eriksen et al., 2014).

Observed MP concentrations of 8–132 particles/fibers m^{-3} (size range: 20 μm–300 μm) for the tropical Indian Ocean are in good accordance with offshore MP number concentrations of 0–300 MP particles/fibers m^{-3} in the Atlantic Ocean as reported by Enders et al. (2015). In their study, MPs were analyzed by Raman spectroscopy (>10 μm) and sampled by fractionated filtration (>10/50 μm) at 3 m below sea-level. Lorenz et al. (2019) took samples (>100 μm) from the southern North Sea and detected 27 ± 53 MPs m^{-3} by means of FPA-based FTIR microspectroscopy. For a meaningful comparison, one should take into account the size detection limit of 11 μm (pixel size), and that MP particles with a size around 11 μm had a share >40%) (Lorenz et al., 2019) (size limit in our study: 20 μm).

Consequently, the tropical Indian Ocean might have significantly higher MP pollution levels than the coastal North Sea, although the latter is more likelyaffected by coastal MP pollution by river run off, ship traffic, tides, and proximity to urban MP sources. MP number concentrations determined for the tropical Indian Ocean are lower than those in subsurface water of northeastern Pacific Ocean including the North Pacific gyre (279 ± 178 MP m^{-3} for particles >62 μm) (Desforges et al., 2014).

3.2.3. Polymer composition

In total, > 56,000 particles were analyzed by means of the automated LDIR workflow. Hereby, 1287 synthetic particles were identified. MPs were grouped in 14 different polymer clusters: acrylates/polyurethane (PU)/varnish (49%), PET (26%), PP (8%), ethylene-vinyl acetate (EVA) (4%), PE (4%), PS (2%), polyvinyl chloride (PVC) (2%), PC (2%), rubber (2%), polyamide (PA) (1%), chlorinated polyethylene (PE-Cl) (<1%), PMMA (<1%), acrylonitrile butadiene (<1%) and silicone (<1%). Manual re-evaluation of MP assignments yielded a false positive rate of <3%, which is similar to the optimized analysis via FTIR microspectroscopy, as published by Primpke et al. (2017) (false positive rate 3.1%). Fig. 3 illustrates the spatial distribution of the polymer composition, combined with a detailed overview of the absolute MP numbers assigned to each polymer type (particles/fibers m^{-3}) for the small MP fraction (20 μm ≤ d ≤ 300 μm). PET was the most abundant polymer type at 5 of 8 stations in the eastern Indian Ocean (stations 1–8), whereas acrylates/PU/varnish was the most abundant polymer cluster at 10 of 13 stations in the western Indian Ocean (stations 9–21). In contrast, PA, PE-Cl PVC, rubber, acrylonitrile butadiene and silicone were found only at station 5 and 14 in the central area of the transect. Up to 11 different MP clusters were detected at station 14. Fig. 3 illustrates the polymeric variabilities of the 21 stations.

Polymer compositions of MPs within the water column are highly affected by density and the state of biofouling. Therefore, sampling of subsurface waters at different water depths may result in selective sampling of plastics by density (Lusher et al., 2014). Additionally, research vessel movement, as well as strong winds and currents may lead to redistribution and mixing of MPs.

In this study, acrylates/PU/varnish account for 15%–83% of all detected MPs and occurred at all stations of the open ocean. Acrylates/PU/varnish abundances are higher at stations located in the western area of the transect (station 13–21) and on average account for 53% of the respective MPs, compared to lower average abundances (37%) for the remaining stations 1–13. Although we have no direct evidence, marine ship traffic (abrasion of particles from ship hull coatings) is likely to be a relevant input source of acrylates/PU/varnish. This group of polymer particles is presumably primarily emitted at sea with a lower contribution by rivers and coastal areas (Haave et al., 2019). PET was detected in all samples with a share ranging from 11% (station 4) to 68% (station 2). The high abundance of PET particles/fibers at some stations may be related to its higher density (ρ = 1.38 g cm^{-3}- 1.41 g cm^{-3}) compared to seawater (ρ = 1.025 g cm^{-3}). Due to their negative

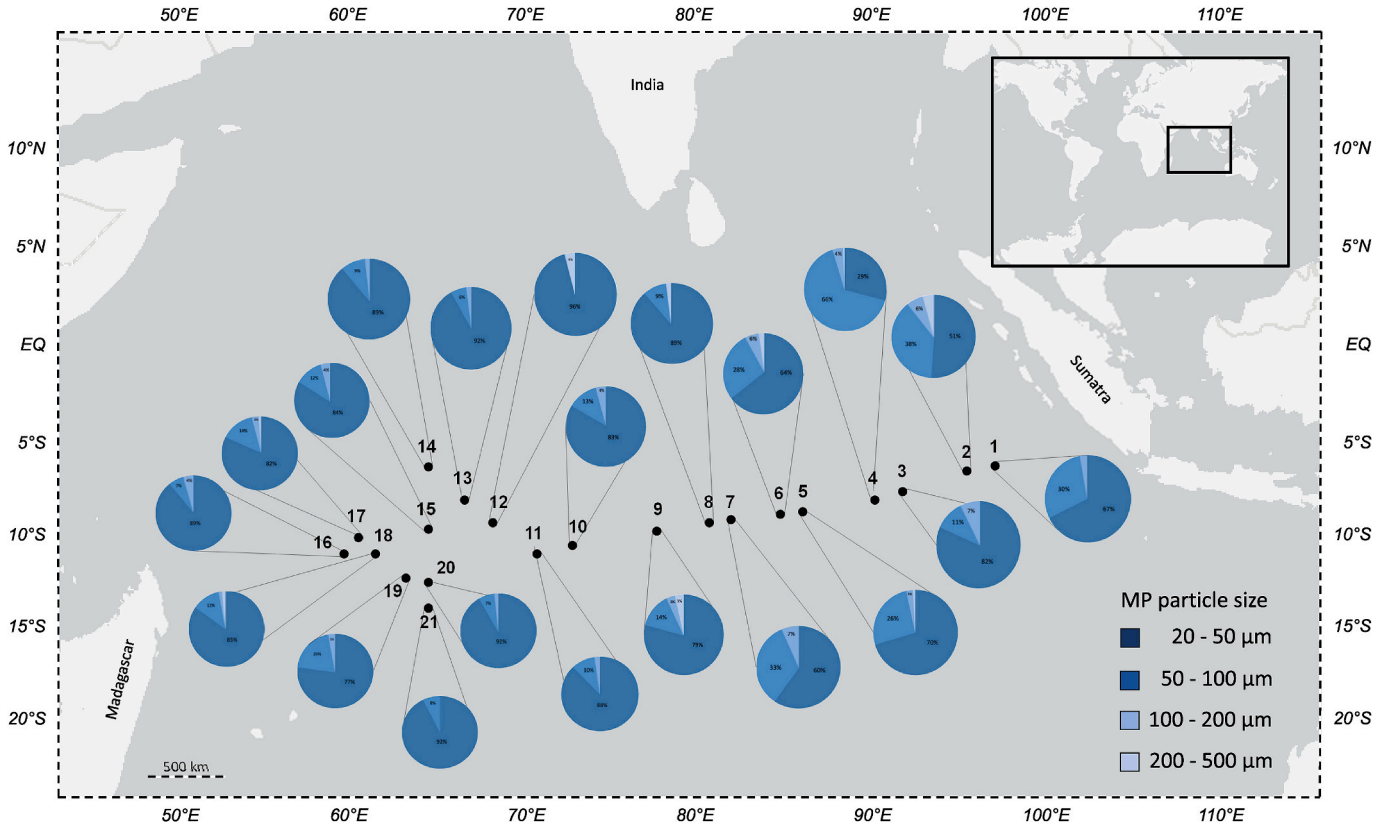

Fig. 4. MP particle size distributions for each station along the tropical Indian Ocean sample transect. Shares <7% are not illustrated.

buoyancy, PET particle concentrations are expected to be high in subsurface waters analyzed in this study.

Despite global high production volumes, PP as well as PE were significantly less abundant than PET in the sample set. However, PP dominated the polymeric compositions of station 3 (40%) and 9 (45%). PP (ρ = 0.85 g cm^{-3} - 0.92 g cm^{-3}) and PE (ρ = 0.89 g cm^{-3}- 0.98 g cm^{-3}) are positively buoyant in seawater and thus expected to float on the sea surface. PP and PE particles/fibers detected in this study were presumably biofilm coated and/or were included into aggregates (marine snow or fecal pellets) that increased particle density.

3.2.4. Particle size distribution

75% of all detected MP particles ($\sum MP_i = 1287$) exhibited particle sizes between 20 μm and 50 μm, followed by 21% in the size range of 50 μm–100 μm, three percent in the size range of 100 μm–200 μm and one percent in the size range of 200 μm–500 μm. A detailed map of the MP size distribution for all samples is presented in Fig. 4. Thus, 96% of all MPs were <100 μm, which is in accordance with other studies. Lorenz et al. (2019) reported that 86% of the MPs were <100 μm. In the study by Haave et al. (2019), over 95% of the detected MP particles were <100 μm. Enders et al. (2015) described an exponential increase in MP quantities with decreasing particle size down to 10 μm. The generally small sizes of MPs underline the necessity to apply appropriate sampling (size cut-off), sample preparation (filter pore sizes, prevention of contamination and particle loss) and analysis methods (advanced chemical microspectroscopy or thermoanalytical methods) to obtain meaningful concentration and size distribution data.

Due to an advanced degree of biofouling, MPs between station 5 and 14 are expected to float for a longer period at sea leading to an advanced degree of MP fragmentation. Along the transect, a distinct trend was observed regarding the particle size distribution. The share of MP particles in the range 50 μm–100 μm decreased and the share of MPs in the range 20 μm–50 μm increased from east to west. This indicates fragmentation taking place along the transect.

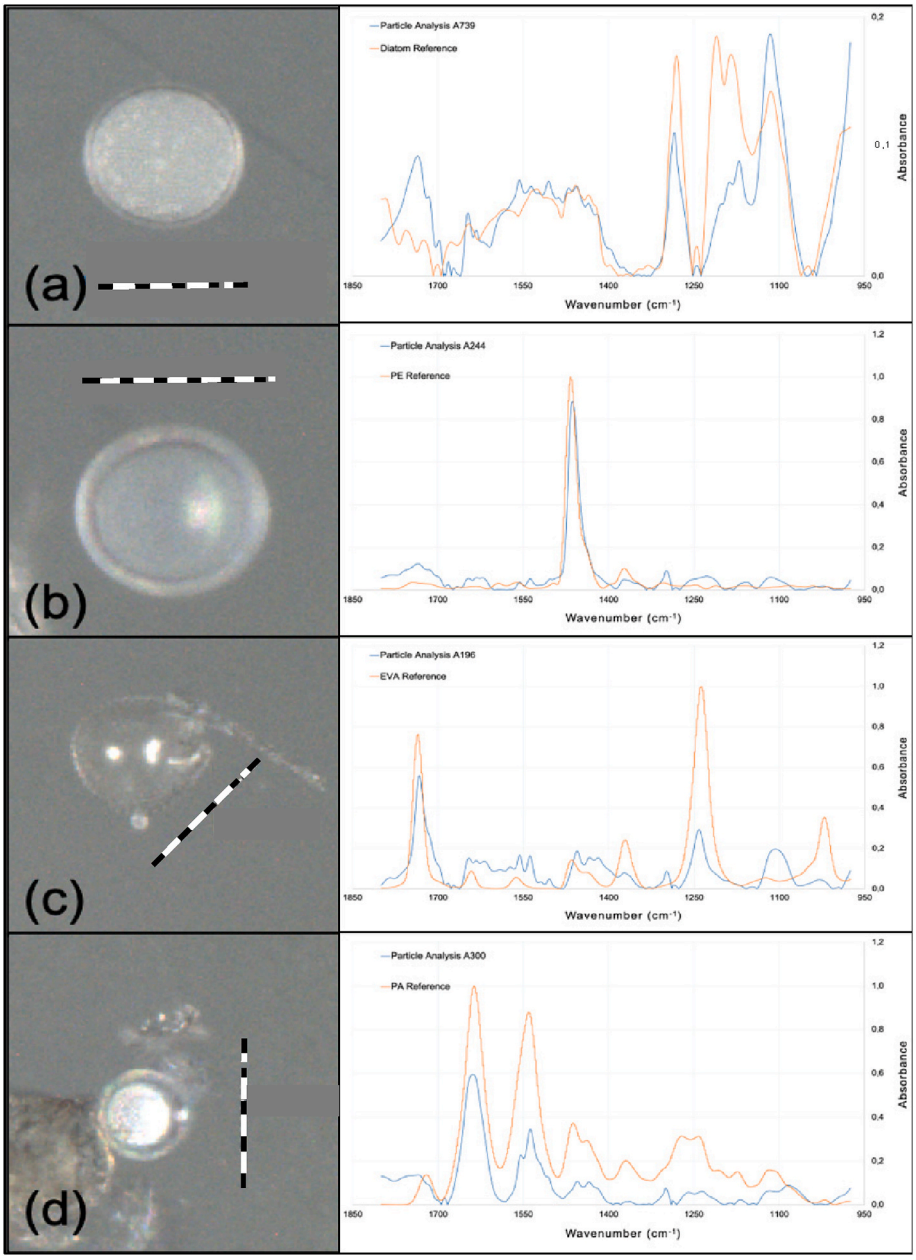

Fig. 5. High magnification images recorded with the LDIR: (a) concentric, natural silica particle; (b) PE microbead; (c) EVA microbead; (d) PA microbead. Scale bars correspond to 50 μm. All spectra were acquired in transflection mode.

The chemical composition of the detected MP particles of the four different size classes (20 μm–50 μm, 50 μm–100 μm, 100 μm–200 μm and 200 μm–500 μm) is shown in SI Fig. 2. Acrylates/PU/varnish dominated the size fraction between 20 μm–50 μm with a share of 51% (over 450 particles) decreasing to 40% (110 particles) with increasing particle size (50 μm–100 μm fraction). This trend continues among the size class 100 μm–200 μm (20%) and the size class 200 μm–500 μm (8%). As already discussed, most particles of the dominating polymer cluster acrylates/PU/varnish presumably originate from marine traffic (Lorenz et al., 2019).

Despite low absolute numbers, PS showed the lowest shares in the size class 20 μm–50 μm (2% and 15 particles), increasing to a share of 4% in the size class 50 μm–100 μm (11 particles). The proportion of PS rises in the size class 100 μm–200 μm to a share of 7% and reaches its maximum share in the size class 200 μm–500 μm with 18%. PP and rubber exhibited higher shares in the size fraction 200 μm–500 μm compared to smaller size fractions. The data indicate that the PS, rubber and PP particles were subjected to the process of biofouling and weathering of larger plastic litter, whose influence might be greater for subsurface locations in the open ocean. PET particles were dominant in the size fraction 100 μm–200 μm with a share of 42%.

3.3. Microbeads

Currently, the accurate differentiation between natural PA and synthetic PA in environmental samples remains challenging. In contrast to the most relevant synthetic polymer types, the covered wavenumber range of the LDIR (1800 cm^{-1} – 975 cm^{-1}) hampered clear assignments to artificial PA. Thus, all synthetic PA particles detected in this study (12 in total) were visually confirmed with the high-magnification-microscope objective of the LDIR system. All PA particles included in this study were microbeads. Other microbeads of different polymeric origin were also identified (PE and EVA), some of them are illustrated in Fig. 5. EVA was almost solely detected in particle size class between 20 μm–50 μm (48 particles). Radial diatoms remaining in the sample and colorless microbeads often had a similar appearance providing good examples why visual identification without chemical imaging is definitely not sufficient for MP analysis.

4. Conclusion

This study provides the first dataset on the occurrence, distribution, polymer types and particle sizes of MPs in the tropical Indian Ocean. To gain a better understanding, further MP studies in the Indian Ocean are certainly needed. Currently, no field-studies are available on MP occurrences in the Indian Ocean Gyre, which is presumably an accumulation hotspot for MPs. Even though inter-study comparison is problematic due to the application of different methods (sampling and detection), the reported concentrations (8–132 MPs m^{-3}) are well in line with other studies, based on either FTIR or Raman microspectroscopy. These results demonstrate once more how particulate plastics have pervaded the aquatic environment. Particle concentrations strongly increase with decreasing particle sizes with >95% of MPs being smaller than 100 μm. Considering that this trend obeys a power law with an exponent between 2 and 3 (Cabernard et al., 2018; Kooi et al., 2021), reported environmental MP concentrations will strongly increase if particles <10 μm or 20 μm (size limit set in this study) can be quantified in a reliable manner.

From the perspective of a routine analysis laboratory, established sample preparation and detection methods are still too labor-intensive, time-consuming and dependent on the operator skills. Therefore, time-efficient, automatable and validated chemical-analytical and data processing workflows are indispensable. Microwave-assisted sample preparation may help to significantly reduce and simplify sample preparation. Advantages over a conventional hot blocks are fast and homogeneous energy supply, accurate temperature control by an IR sensor, fast cooling (if required), usage of an autosampler and automated stirring. Procedural contamination and sample loss were minimized by a temporary “one-pot” matrix digestion approach (only 4 filtration steps).

The results stress the high future potential of LDIR imaging for time-efficient and automated MP analysis. For the MP fraction >300 μm, very good agreement was achieved between ATR-FTIR analysis and LDIR imaging. Despite a low share of false positive assignments (<3%) for MPs <300 μm, extension of the database by typical matrix spectra and further improvements of the instrument’s software (more accurate and smoother image collection) will help to further increase the accuracy of the automated MP workflow. The opportunity to apply the automated MP workflow to filter membranes, e.g., of Au-coated PC, would also be highly beneficial as transferring entire samples onto MirrIR slides is prone to particle loss, while subsampling can cause significant bias (López-Rosales et al., 2022). Scientists have already applied LDIR imaging to determine very high MP concentrations (20–3368 μm, 520 and 430 MP g^{-1}) in two sediment samples from Lake Michigan (Cheng et al., 2021). To our knowledge, the presented work contains the most comprehensive application and validation of LDIR imaging for environmental MP analysis so far.

Author statement

LH: Conceptualization, Methodology, Investigation, Validation, Writing – original draft. **FEG**: Methodology, Validation, Investigation, Writing – original draft. **TZ**: Conceptualization, Methodology, Writing – original draft, Writing – review & editing. **OK**: Formal analysis, Data curation. **AK**: Methodology. **KCE**: Resources, Writing – review & editing, Supervision. **DP**: Conceptualization, Resources, Writing – review & editing, Supervision.

Declaration of competing interest

The authors declare that they have no known competing financial interests or personal relationships that could have appeared to influence the work reported in this paper.

Acknowledgement

The authors would like to thank Silvio Neumann from the providing access to an ATR-FTIR unit, Dr. Martin Held and Anke-Lisa Höhme for the SEM analysis of model polymer particles, Dr. Thomas Emmler (all from the Institute of Membrane Research, Helmholtz-Zentrum Hereon) for the Raman analysis of a suspected MP fiber and Dr. Dieter Fischer from the Leibniz-Institut für Polymerforschung Dresden for the subsequent database research of the generated Raman spectrum. Captain and crew of r/v SONNE are acknowledged for expert support at sea. This study was funded by BMBF through grant 03G0270A.

Appendix A. Supplementary data

Supplementary data to this article can be found online at https://doi.org/10.1016/j.envpol.2022.119547.

References

Agarwal, V., Kaur, R., De, D., 2017. Scenario analysis of textile industry in Asia-Pacific trade agreement (APTA). Procedia Comput. Sci. 122, 685–690.

Bannick, C.G., Szewzyk, R., Ricking, M., Schniegler, S., Obermaier, N., Barthel, A.K., Altmann, K., Eisentraut, P., Braun, U., 2019. Development and testing of a fractionated filtration for sampling of microplastics in water. Water Res. 149, 650–658.

Becker, R., Altmann, K., Sommerfeld, T., Braun, U., 2020. Quantification of microplastics in a freshwater suspended organic matter using different thermoanalytical methods – outcome of an interlaboratory comparison. J. Anal. Appl. Pyrol. 148, 104829.

Bergmann, M., Wirzberger, V., Krumpen, T., Lorenz, C., Primpke, S., Tekman, M.B., Gerdts, G., 2017. High quantities of microplastic in arctic deep-sea sediments from the HAUSGARTEN observatory. Environ. Sci. Technol. 51 (19), 11000–11010.
Bordós, G., Gergely, S., Háhn, J., Palotai, Z., Szabó, É., Besenyő, G., Salgó, A., Harkai, P., Kriszt, B., Szoboszlay, S., 2021. Validation of pressurized fractionated filtration microplastic sampling in controlled test environment. Water Res. 189, 116572.
Brahney, J., Mahowald, N., Prank, M., Cornwell, G., Klimont, Z., Matsui, H., Prather, K. A., 2021. Constraining the atmospheric limb of the plastic cycle. Proc. Natl. Acad. Sci. Unit. States Am. 118 (16), e2020719118.
Burns, E.E., Boxall, A.B.A., 2018. Microplastics in the aquatic environment: evidence for or against adverse impacts and major knowledge gaps. Environ. Toxicol. Chem. 37 (11), 2776–2796.
Cheng, Y.-L., Zhang, R., Tisinger, L., Cali, S., Yu, Z., Chen, H.Y., Li, A., 2021. Characterization of microplastics in sediment using stereomicroscopy and laser direct infrared (LDIR) spectroscopy. Gondwana Res. https://doi.org/10.1016/j.gr.2021.10.002. In press.
Childs, D.T.D., Hogg, R.A., Revin, D.G., Rehman, I.U., Cockburn, J.W., Matcher, S.J., 2015. Sensitivity advantage of QCL tunable-laser mid-infrared spectroscopy over FTIR spectroscopy. Appl. Spectrosc. Rev. 50 (10), 822–839.
Cole, M., 2016. A novel method for preparing microplastic fibers. Sci. Rep. 6 (1), 34519.
Coppock, R.L., Cole, M., Lindeque, P.K., Queirós, A.M., Galloway, T.S., 2017. A small-scale, portable method for extracting microplastics from marine sediments. Environ. Pollut. 230, 829–837.
Cutroneo, L., Reboa, A., Besio, G., Borgogno, F., Canesi, L., Canuto, S., Dara, M., Enrile, F., Forioso, I., Greco, G., Lenoble, V., Malatesta, A., Mounier, S., Petrillo, M., Rovetta, R., Stocchino, A., Tesan, J., Vagge, G., Capello, M., 2020. Microplastics in seawater: sampling strategies, laboratory methodologies, and identification techniques applied to port environment. Environ. Sci. Pollut. Control Ser. 27 (9), 8938–8952.
da Costa Filho, P.A., Cobuccio, L., Mainali, D., Rault, M., Cavin, C., 2020. Rapid analysis of food raw materials adulteration using laser direct infrared spectroscopy and imaging. Food Control 113, 107114.
Desforges, J.-P.W., Galbraith, M., Dangerfield, N., Ross, P.S., 2014. Widespread distribution of microplastics in subsurface seawater in the NE Pacific Ocean. Mar. Pollut. Bull. 79 (1), 94–99.
Dimante-Deimantovica, I., Suhareva, N., Barone, M., Putna-Nimane, I., Aigars, J., 2022. Hide-and-seek: threshold values and contribution towards better understanding of recovery rate in microplastic research. MethodsX 9, 101603.
Dong, M., She, Z., Xiong, X., Ouyang, G., Luo, Z., 2022. Automated analysis of microplastics based on vibrational spectroscopy: are we measuring the same metrics? Anal. Bioanal. Chem. 414 (11), 3359–3372.
Doulamis, A., Doulamis, N., Angeli, A., Lazaris, A., Luthman, S., Jayapala, M., Silbernagel, G., Napp, A., Lazarou, I., Karalis, A., Hoveling, R., Terzopoulos, P., Yamas, A., Georgiadis, P., Maulini, R., Muller, A., 2021. A non-invasive photonics-based device for monitoring of diabetic foot ulcers: architectural/sensorial components & technical specifications. Inventions 6, 27.
Doyle, M.J., Watson, W., Bowlin, N.M., Sheavly, S.B., 2011. Plastic particles in coastal pelagic ecosystems of the Northeast Pacific ocean. Mar. Environ. Res. 71 (1), 41–52.
Dris, R., Gasperi, J., Saad, M., Mirande, C., Tassin, B., 2016. Synthetic fibers in atmospheric fallout: a source of microplastics in the environment? Mar. Pollut. Bull. 104 (1), 290–293.
Duemichen, E., Eisentraut, P., Celina, M., Braun, U., 2019. Automated thermal extraction-desorption gas chromatography mass spectrometry: a multifunctional tool for comprehensive characterization of polymers and their degradation products. J. Chromatogr. A 1592, 133–142.
Enders, K., Lenz, R., Stedmon, C.A., Nielsen, T.G., 2015. Abundance, size and polymer composition of marine microplastics ≥10μm in the Atlantic Ocean and their modelled vertical distribution. Mar. Pollut. Bull. 100 (1), 70–81.
Eriksen, M., Lebreton, L.C., Carson, H.S., Thiel, M., Moore, C.J., Borerro, J.C., Galgani, F., Ryan, P.G., Reisser, J., 2014. Plastic pollution in the world's oceans: more than 5 trillion plastic pieces weighing over 250,000 tons afloat at sea. PLoS One 9 (12), e111913.
European Chemical Agency, 2019. Restricting the Use of Intentionally Added Microplastic Particles to Consumer or Professional Use Products of Any Kind, 2019.
Fischer, M., Scholz-Böttcher, B.M., 2017. Simultaneous trace identification and quantification of common types of microplastics in environmental samples by pyrolysis-gas chromatography–mass spectrometry. Environ. Sci. Technol. 51 (9), 5052–5060.
Frias, J.P.G.L., Nash, R., 2019. Microplastics: finding a consensus on the definition. Mar. Pollut. Bull. 138, 145–147.
Funck, M., Yildirim, A., Nickel, C., Schram, J., Schmidt, T.C., Tuerk, J., 2020. Identification of microplastics in wastewater after cascade filtration using Pyrolysis-GC–MS. MethodsX 7, 100778.
Haave, M., Lorenz, C., Primpke, S., Gerdts, G., 2019. Different stories told by small and large microplastics in sediment - first report of microplastic concentrations in an urban recipient in Norway. Mar. Pollut. Bull. 141, 501–513.
Henry, B., Laitala, K., Klepp, I.G., 2019. Microfibres from apparel and home textiles: prospects for including microplastics in environmental sustainability assessment. Sci. Total Environ. 652, 483–494.
Hildebrandt, L., Gareb, F., Zimmermann, T., Klein, O., Emeis, K., Kerstan, A., Pröfrock, D., 2020a. Agilent Application Note: Fast, Automated Microplastics Analysis Using Laser Direct Chemical Imaging - Characterizing and Quantifying Microplastics in Water Samples from Marine Environments.
Hildebrandt, L., Mitrano, D.M., Zimmermann, T., Pröfrock, D., 2020b. A nanoplastic sampling and enrichment approach by continuous flow centrifugation. Front. Environ. Sci. 8 (89).
Hildebrandt, L., Nack, F.L., Zimmermann, T., Pröfrock, D., 2021. Microplastics as a Trojan horse for trace metals. J. Hazard. Mater. Lett. 2, 100035.
Hildebrandt, L., Voigt, N., Zimmermann, T., Reese, A., Proefrock, D., 2019. Evaluation of continuous flow centrifugation as an alternative technique to sample microplastic from water bodies. Mar. Environ. Res. 151, 104768.
Hüffer, T., Praetorius, A., Wagner, S., von der Kammer, F., Hofmann, T., 2017. Microplastic exposure assessment in aquatic environments: learning from similarities and differences to engineered nanoparticles. Environ. Sci. Technol. 51 (5), 2499–2507.
Huppertsberg, S., Knepper, T.P., 2018. Instrumental analysis of microplastics—benefits and challenges. Anal. Bioanal. Chem. 410 (25), 6343–6352.
Karami, A., Golieskardi, A., Choo, C.K., Romano, N., Ho, Y.B., Salamatinia, B., 2017. A high-performance protocol for extraction of microplastics in fish. Sci. Total Environ. 578, 485–494.
Karlsson, T.M., Kärrman, A., Rotander, A., Hassellöv, M., 2020. Comparison between manta trawl and in situ pump filtration methods, and guidance for visual identification of microplastics in surface waters. Environ. Sci. Pollut. Control Ser. 27 (5), 5559–5571.
Kirstein, I.V., Hensel, F., Gomiero, A., Iordachescu, L., Vianello, A., Wittgren, H.B., Vollertsen, J., 2021. Drinking plastics? – quantification and qualification of microplastics in drinking water distribution systems by μFTIR and Py-GCMS. Water Res. 188, 116519.
Koelmans, A.A., Mohamed Nor, N.H., Hermsen, E., Kooi, M., Mintenig, S.M., De France, J., 2019. Microplastics in freshwaters and drinking water: critical review and assessment of data quality. Water Res. 155, 410–422.
Kooi, M., Reisser, J., Slat, B., Ferrari, F.F., Schmid, M.S., Cunsolo, S., Brambini, R., Noble, K., Sirks, L.-A., Linders, T.E.W., Schoeneich-Argent, R.I., Koelmans, A.A., 2016. The effect of particle properties on the depth profile of buoyant plastics in the ocean. Sci. Rep. 6 (1), 33882.
Kuepper, C., Kallenbach-Thieltges, A., Juette, H., Tannapfel, A., Großerueschkamp, F., Gerwert, K., 2018. Quantum cascade laser-based infrared microscopy for label-free and automated cancer classification in tissue sections. Sci. Rep. 8 (1), 7717.
Li, C., Wang, X., Liu, K., Zhu, L., Wei, N., Zong, C., Li, D., 2021a. Pelagic microplastics in surface water of the Eastern Indian Ocean during monsoon transition period: abundance, distribution, and characteristics. Sci. Total Environ. 755, 142629.
Li, D., Liu, K., Li, C., Peng, G., Andrady, A.L., Wu, T., Zhang, Z., Wang, X., Song, Z., Zong, C., Zhang, F., Wei, N., Bai, M., Zhu, L., Xu, J., Wu, H., Wang, L., Chang, S., Zhu, W., 2020. Profiling the vertical transport of microplastics in the west Pacific Ocean and the east Indian ocean with a novel in situ filtration technique. Environ. Sci. Technol. 54 (20), 12979–12988.
Li, L., Zhao, X., Li, Z., Song, K., 2021b. COVID-19: performance study of microplastic inhalation risk posed by wearing masks. J. Hazard Mater. 411, 124955.
Löder, M.G.J., Imhof, H.K., Ladehoff, M., Löschel, L.A., Lorenz, C., Mintenig, S., Piehl, S., Primpke, S., Schrank, I., Laforsch, C., Gerdts, G., 2017. Enzymatic purification of microplastics in environmental samples. Environ. Sci. Technol. 51 (24), 14283–14292.
López-Rosales, A., Andrade, J., Fernández-González, V., López-Mahía, P., Muniategui-Lorenzo, S., 2022. A reliable method for the isolation and characterization of microplastics in fish gastrointestinal tracts using an infrared tunable quantum cascade laser system. Mar. Pollut. Bull. 178, 113591.
Lorenz, C., Roscher, L., Meyer, M.S., Hildebrandt, L., Prume, J., Löder, M.G.J., Primpke, S., Gerdts, G., 2019. Spatial distribution of microplastics in sediments and surface waters of the southern North Sea. Environ. Pollut. 252, 1719–1729.
Lusher, A.L., Burke, A., O'Connor, I., Officer, R., 2014. Microplastic pollution in the Northeast Atlantic Ocean: validated and opportunistic sampling. Mar. Pollut. Bull. 88 (1), 325–333.
Mai, L., Bao, L.-J., Wong, C.S., Zeng, E.Y., 2018. In: Zeng, E.Y. (Ed.), Microplastic Contamination in Aquatic Environments. Elsevier, pp. 365–378.
Mani, T., Hauk, A., Walter, U., Burkhardt-Holm, P., 2015. Microplastics profile along the rhine river. Sci. Rep. 5 (1), 17988.
Miller, M.E., Kroon, F.J., Motti, C.A., 2017. Recovering microplastics from marine samples: a review of current practices. Mar. Pollut. Bull. 123 (1), 6–18.
Mitrano, D.M., Beltzung, A., Frehland, S., Schmiedgruber, M., Cingolani, A., Schmidt, F., 2019. Synthesis of metal-doped nanoplastics and their utility to investigate fate and behaviour in complex environmental systems. Nat. Nanotechnol. 14 (4), 362–368.
Mitrano, D.M., Wohlleben, W., 2020. Microplastic regulation should be more precise to incentivize both innovation and environmental safety. Nat. Commun. 11 (1), 5324.
Möller, J.N., Heisel, I., Satzger, A., Vizsolyi, E.C., Oster, S.D.J., Agarwal, S., Laforsch, C., Löder, M.G.J., 2022. Tackling the challenge of extracting microplastics from soils: a protocol to purify soil samples for spectroscopic analysis. Environ. Toxicol. Chem. 41 (4), 844–857.
Müller, Y.K., Wernicke, T., Pittroff, M., Witzig, C.S., Storck, F.R., Klinger, J., Zumbülte, N., 2020. Microplastic analysis—are we measuring the same? Results on the first global comparative study for microplastic analysis in a water sample. Anal. Bioanal. Chem. 412 (3), 555–560.
Munno, K., Helm, P.A., Jackson, D.A., Rochman, C., Sims, A., 2018. Impacts of temperature and selected chemical digestion methods on microplastic particles. Environ. Toxicol. Chem. 37 (1), 91–98.
Ogunleke, A., Bobroff, V., Chen, H.-H., Rowlette, J., Delugin, M., Recur, B., Hwu, Y., Petibois, C., 2017. Fourier-transform vs. quantum-cascade-laser infrared microscopes for histo-pathology: from lab to hospital? Trac. Trends Anal. Chem. 89, 190–196.
Patti, T.B., Fobert, E.K., Reeves, S.E., Burke da Silva, K., 2020. Spatial distribution of microplastics around an inhabited coral island in the Maldives, Indian Ocean. Sci. Total Environ. 748, 141263.

Prata, J.C., Reis, V., da Costa, J.P., Mouneyrac, C., Duarte, A.C., Rocha-Santos, T., 2021. Contamination issues as a challenge in quality control and quality assurance in microplastics analytics. J. Hazard Mater. 403, 123660.
Primpke, S., Cross, R.K., Mintenig, S.M., Simon, M., Vianello, A., Gerdts, G., Vollertsen, J., 2020a. Toward the systematic identification of microplastics in the environment: evaluation of a new independent software tool (siMPle) for spectroscopic analysis. Appl. Spectrosc. 74 (9), 1127–1138.
Primpke, S., Godejohann, M., Gerdts, G., 2020b. Rapid identification and quantification of microplastics in the environment by quantum cascade laser-based hyperspectral infrared chemical imaging. Environ. Sci. Technol. 54 (24), 15893–15903.
Primpke, S., Lorenz, C., Rascher-Friesenhausen, R., Gerdts, G., 2017. An automated approach for microplastics analysis using focal plane array (FPA) FTIR microscopy and image analysis. Anal. Methods 9 (9), 1499–1511.
Reineccius, J., Appelt, J.S., Hinrichs, T., Kaiser, D., Stern, J., Prien, R.D., Waniek, J.J., 2020. Abundance and characteristics of microfibers detected in sediment trap material from the deep subtropical North Atlantic Ocean. Sci. Total Environ. 738, 140354.
Scherer, C., Weber, A., Stock, F., Vurusic, S., Egerci, H., Kochleus, C., Arendt, N., Foeldi, C., Dierkes, G., Wagner, M., Brennholt, N., Reifferscheid, G., 2020. Comparative assessment of microplastics in water and sediment of a large European river. Sci. Total Environ. 738, 139866.
Scheurer, M., Bigalke, M., 2018. Microplastics in Swiss floodplain soils. Environ. Sci. Technol. 52 (6), 3591–3598.
Schmidt, C., Krauth, T., Wagner, S., 2017. Export of plastic debris by rivers into the sea. Environ. Sci. Technol. 51 (21), 12246–12253.
Scircle, A., Cizdziel, J.V., Tisinger, L., Anumol, T., Robey, D., 2020. Occurrence of microplastic pollution at oyster reefs and other coastal sites in the Mississippi sound, USA: impacts of freshwater inflows from flooding. Toxics 8 (2).
Song, Y.K., Hong, S.H., Jang, M., Han, G.M., Jung, S.W., Shim, W.J., 2017. Combined effects of UV exposure duration and mechanical abrasion on microplastic fragmentation by polymer type. Environ. Sci. Technol. 51 (8), 4368–4376.
Stock, F., Narayana, V.K.B., Scherer, C., Löder, M.G.J., Brennholt, N., Laforsch, C., Reifferscheid, G., 2020. Pitfalls and Limitations in Microplastic Analyses. Springer Berlin Heidelberg, Berlin, Heidelberg, pp. 1–30.
Suaria, G., Achtypi, A., Perold, V., Lee, J.R., Pierucci, A., Bornman, T.G., Aliani, S., Ryan, P.G., 2020. Microfibers in oceanic surface waters: a global characterization. Sci. Adv. 6 (23), eaay8493.
Tamminga, M., Stoewer, S.-C., Fischer, E.K., 2019. On the representativeness of pump water samples versus manta sampling in microplastic analysis. Environ. Pollut. 254, 112970.
Thiele, C.J., Hudson, M.D., Russell, A.E., 2019. Evaluation of existing methods to extract microplastics from bivalve tissue: adapted KOH digestion protocol improves filtration at single-digit pore size. Mar. Pollut. Bull. 142, 384–393.
Thiele, C.J., Hudson, M.D., Russell, A.E., Saluveer, M., Sidaoui-Haddad, G., 2021. Microplastics in fish and fishmeal: an emerging environmental challenge? Sci. Rep. 11 (1), 2045.
van der Mheen, M., van Sebille, E., Pattiaratchi, C., 2020. Beaching patterns of plastic debris along the Indian Ocean rim. Ocean Sci. 16 (5), 1317–1336.
Walker, T.R., 2021. Micro)plastics and the UN sustainable development Goals. Curr. Opin. Green Sustain. Chem. 30, 100497.
Wang, Z., Taylor, S.E., Sharma, P., Flury, M., 2018. Poor extraction efficiencies of polystyrene nano- and microplastics from biosolids and soil. PLoS One 13 (11) e0208009-e0208009.
Wesch, C., Elert, A.M., Wörner, M., Braun, U., Klein, R., Paulus, M., 2017. Assuring quality in microplastic monitoring: about the value of clean-air devices as essentials for verified data. Sci. Rep. 7 (1), 5424.